Population Density Measurements in a Supersonic Freejet Expansion Flow of an O₂-seeded Ar Plasma

By

Akira KIMURA*, Masahiro MINOMO** and Michio NISHIDA***

(Received September 27, 1979)

Abstract

The population densities of $O(3p^3P)$ and $O(3p^5P)$ were measured along the freejet centerline of an O_2-seeded Ar plasma, which was such that oxygen gas was seeded into a pre-ionized argon plasma. The ratio of the measured population densities of the $3p^3P$ and $3p^5P$ states was compared with the predicted ratio, which was determined from a steady state population assumption of $O(3p^5P)$, over the whole region of the freejet. The comparison showed that on the condition $N_e = 1.8 \times 10^{13} - 1.7 \times 10^{12} cm^{-3}$, $T_e = 3000 - 900$ K and $p = 48 - 0.19$ Pa, the $3p^5P$ state is populated by electron-collisional de-excitations of the $3p^3P$ state, rather than by quenching of the $3p^3P$ state by the ground state argon. Further, the $3p^5P$ state is de-populated by electron-collisional de-excitations rather than by radiative de-excitations.

1. Introduction

Since the work made by Bennett et al.[1], there has been considerable interest in electronic energy transfer from metastable argon to oxygen[2,3]. Quenching of the metastable Ar* by ground state O_2 is accompanied with the dissociation of O_2 into $O(2p^4 \, ^3P)$ and $O(2p^4 \, ^1S$ or $2p^4 \, ^1D)$. Also the quenching of Ar* by $O(2p^4 \, ^3P)$ is followed by the excitation of $O(2p^4 \, ^3P)$ into the $3p^3P$ state. Collisions of $O(3p^3P)$ with the ground state Ar cause de-excitation $3p^3P \rightarrow 3p^5P$ populates the $3p^5P$ state. In addition, electron-collisional transitions should be considered. The present experiment has been concerned with obtaining the population densities of $O(3p^3P)$ and $O(3p^5P)$, which are produced through the above processes. Masurements have been made on the lines of OI8446

* Laboratoire de Thermodynamique, Faculté des Sciences, Université de Rouen, 76130 Mont-Saint-Aignan, France. (Former Graduate Student of Aeronautical Engineering Course.)
** Yokosuka Electrical Communication Laboratory, Nippon Telegraph and Telephone Public Corporation. (Former Graduate Student of Aeronautical Engineering Course.)
*** Department of Aeronautical Engineering.

and OI773, which originate from the transition $3p^3P-3s^3S^0$ and $3p^5P-3s^5S^0$, respectively. For the sake of obtaining experimental data in the condition of low pressure but relatively high electron density, the measurements have been made in a supersonic freejet of an ionized gas produced by an arc discharge.   In addition, experimental data over a wide range of the freejet pressure and electron density can be obtained from the freejet experiment, since the freejet is a rapidly expanding flow.

2. Experimental Apparatus and Procedure

2. 1. Plasma Facility

The experiment has been carried out in a low-density plasma facility operated by a d. c. arc discharge.   The performance of this facility is described in detail in Ref. 4. A schematic diagram of an operating system is shown in Fig. 1.   The test section consists of a cylinder, 18cm in diameter and 110cm in length, and is connected with a 2600 liters vacunm tank.   The argon gas, which is heated and partially ionized by an arc heater with a maximum power of 25kw, flows into a plenum chamber, where the oxygen gas is seeded ($[O_2]/[Ar] \simeq 1/40$).   The gas mixture of argon and oxygen expands through an orifice with a diameter of 13. 7mm into a test section as a supersonic freejet. For the purpose of making spectroscopic measurements in a fixed optical system, the position of the orifice relative to the optical axis can be conveniently moved as shown in Fig. 1.

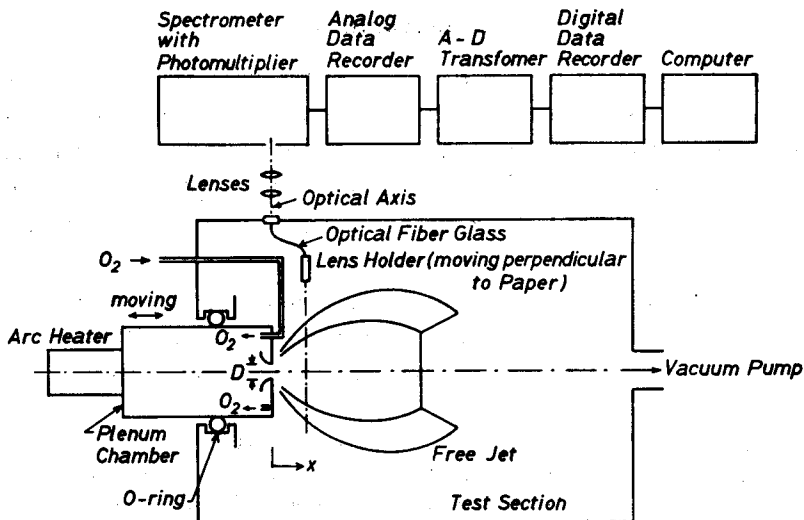Typical operating conditions are as follows: the argon mass flow rate is 0. 11 gr/

Fig. 1. Schematic diagram of measurement.

sec, the stagnation pressure (≃plenum chamber pressure) 1800 Pa (13.5 Torr), the test section pressure 10 Pa (0.075 Torr) and the stagnation temperatute 3400K. First of all, the impact pressure has been measured along the freejet centerline. The Mach number distribution in the freejet has been determined from the impact pressure and the stagnation pressure. Using an isentropic relation, the freejet pressure has been calculated from the stagnation pressure.

2.2. Electrostatic Probe Measurements

The electron temperature and density have been measured by means of a conventional plane electrostatic probe which was made of tungsten, 0.5mm in diameter. The collecting surface of the probe has been mounted parallel to the freejet axis. 20 saw-tooth signals have been used as a probe voltage. The probe current and probe voltage signals have been recorded by an analogue data recorder, and converted to digital data which have been given to a computer. In order to improve the accuracy of the data processing, a statistical method has been employed. The statistical processing method is the so called "M-estimation" method, which is one of the "Robust Estimation Methods." A detailed explanation of this method can be found in Ref. 5.

2.3. Spectroscopic Measurements

The schematic diagram of the spectroscopic measurements is also shown in Fig. 1. For the sake of determining the true values of the intensities on the freejet centerline by means of an Abel inversion[6], a radial survey of spectrum must be carried out. For this purpose an optic fiber glass has been employed, which brings the light emitted perpendicularly to the freejet axis to the entrance slit of a spectrometer. (Shimadzu GCT-100 plane diffraction grating spectrograph with a range of wave lengths 2000 A–9000 A, focal distance of the main concave mirror 100cm, grating number of 1200cm⁻¹, grating area of 102×102mm² and first order inverse dispersion 7.7A/mm. It is equipped with two photomultipliers.) As shown in Fig. 2, a lens in the light
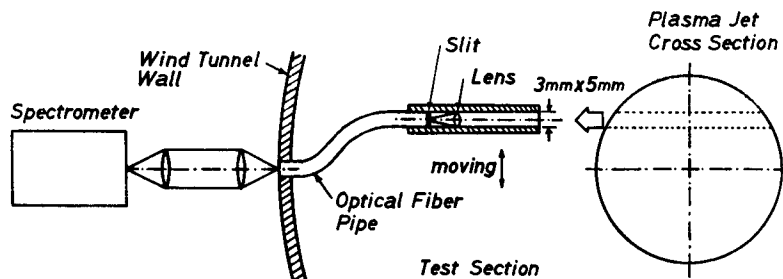

Fig. 2. Optical system.

guide pipe with a 3mm × 5mm cross section focuses the light on the end surface of the optic fiber glass.   The slit placed immediately ahead of the end surface selects only the light parallel to the light guide pipe which is carefully mounted perpendicularly to the freejet axis.   The emission intensities are detected by the photomultipliers and the outputs are recorded on a magnetic tape, which gives the data to a computer.   The optical system has been calibrated for absolute intensity measurements by using a standard tungsten ribbon filament lamp.   The calibration data have been also given to the computer.   After the Abel inversion on the computer, the absolute values of the population density on the freejet centerline have been determined.

The absolute population densities have been obtained as follows: If the self-absorption of a plasma is negligible, the total intensity of line spectrum $I_{j,k}$, which corresponds to a transition from the j-state to the k-state, is proportional to the total population density of an upper state of the transition $j \rightarrow k$ and is expressed as

$$I_{j,k} = C A_{j,k} h \nu_{j,k} N(j),$$ (1)

where C is the calibration factor for the optical system, $A_{j,k}$ the Einstein A coefficient for a radiative transition $j \rightarrow k$, h Plankc's constant, $\nu_{j,k}$ the frequency of the corresponding spectrum and $N(j)$ the population density of the j-state.   For the sake of estimating the absolute population density, the intensity calibration for the optical system must be made with a standard tungsten ribbon filament lamp.   Then the calibrated line intensity $I'_{j,k}$ is expressed as

$$I'_{j,k} = (I_b / I_t) I^m_{j,k},$$ (2)

where I_t is the output intensity signal of the tungsten lamp, measured in the same optical system as used in the measurements of the line intensity $I^m_{j,k}$ from the plasma. I_b is the intensity of the radiation emitted from the tungsten lamp, which is given by

$$I_b = \tau_0 E(\lambda, T_t) C_1 \lambda^{-5} \exp(-C_2 / \lambda T_t) \Delta\lambda,$$ (3)

where τ_0 is the transmissivity of the lamp which was taken to be 0.9, $E(\lambda, T_t)$ the radiative emissivity of the lamp which is given in Ref. 7, C_1 the first radiation constant ($= 0.3742 \times 10^{-4}$ erg cm² sec⁻¹), C_2 the second radiation constant ($= 1.439$ cm K), $\Delta\lambda$ the wave length width through the exit slit and T_t the real temperature of the lamp.   Since it follows that the constant C in Eq. (1) is equal to I_t / I_b, we have

$$N(j) = \frac{1}{A_{j,k} h \nu_{j,k}} \frac{I_b}{I_t} I^m_{j,k}.$$ (4)

3. Results and Discussions

3. 1. Freejet Pressure

In Fig. 3 is shown the freejet pressure variation along the freejet centerline, which has been determined from the stagnation pressure by using the isentropic expansion relation. The freejet pressure varies from 48 Pa (0. 36 Torr) at $x/D=1.1$ to 0. 19 Pa (0. 0014 Torr) at $x/D=5.1$, where x is the distance from the orifice and D is the orifice diameter (=13. 7mm). The calculated atom density varies from 4.2×10^{15}cm^{-3} at $x/D=1.1$ to 1 5×10^{14}cm^{-3} at $x/D=5.1$.
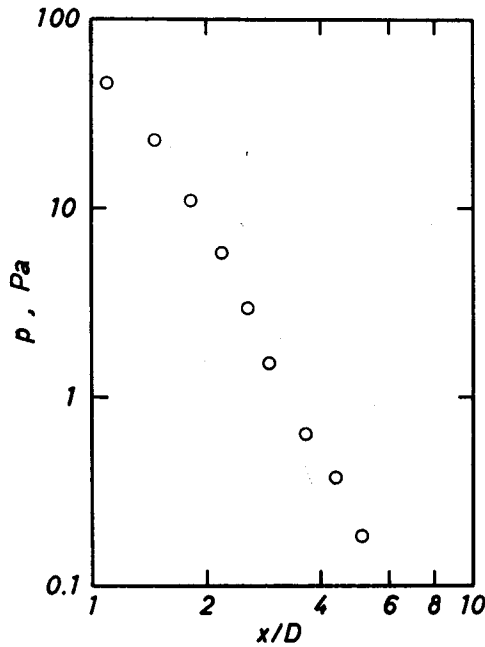

Fig. 3. Axial distribution of pressure on the freejet centerline.

3. 2. Electron Temperature and Density

The electron temperature and density have been measured for both the pure Ar plasma and the O₂-seeded Ar plasma. The results of the electron temperature are shown in Fig. 4. It is obvious that the electron temperature decreases when the oxygen gas is seeded. Immediately after the oxygen gas is seeded into the argon plasma, electrons collide with atomic oxygen which is dissociated by Ar*-O₂ collisions, with the result of excitation of the atomic oxygen. Consequently, the electrons lose their kinetic energy, which is converted to the excitation energy of the atomic oxygen.
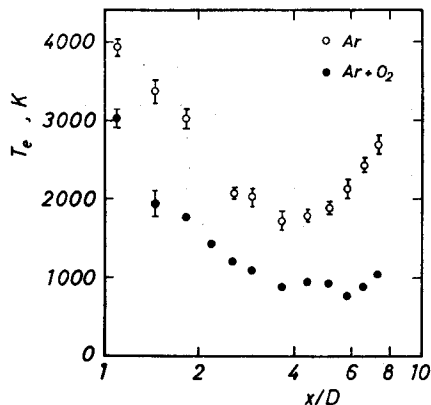
Fig. 4.   Distribution of electron temperature
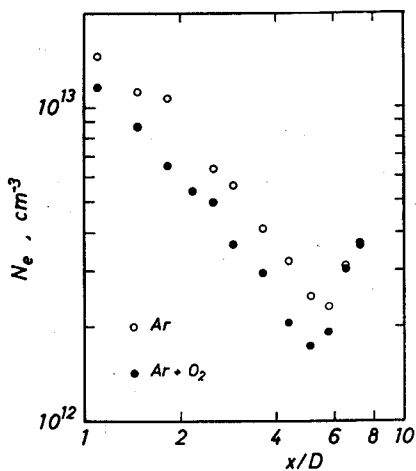   on the freejet centerline.

Fig. 5.   Distribution of electron density on
          the freejet centerline.

The increase in the electron temperature in the downstream is presumably owing to a thermal layer of the elctrons spreading ahead of the Mach disk[8].

Figure 5 illustrates the measured electron density along the freejet centerline for both the pure Ar plasma and O_2-seeded Ar plasma. The result shows that the plasma decays by adding the oxygen gas into the Ar plasma. The increase in the electron density in the downstream of $x/D \simeq 6$ is due to a Mach disk compression.

3.3   Population Densities of Ar($5p[5/2]$) and Ar($5p[3/2]$)

In Fig. 6 are shown the axial distribution of the population densities of Ar($5p[5/2]$) together with the result in the case of the pure Ar plasma. The population densities of the $5p[5/2]$ state have been obtainen from the measurement made on the line of ArI 4300. The decay of the populations is clearly observed when the oxygen gas is seeded. In the cases of the pure Ar plasma and the O_2-seeded plasma, the variation of the population density represents a more gradual decrease than that due to the isentropic expanston. In the downstream of $x/D \simeq 2$ there is much more rapid decease than that due to the isentropic expansion. In the pure argon plasma, the region of the rapid decrease in the population density coincides with that of the increase in the electron temperature shown in Fig. 4. This rapid decrease can be explained as a so called "dark space"[9], which is generally observed ahead of a shock wave of an ionized gas. The rapid decrease in the case of the O_2-seeded Ar plasma is also observed. This is also presumably a dark space, though in Fig. 4 an elevation of the electron temperature in the downstream is not so remarkably observed. The increase in the population density in the downstream represents a compression due
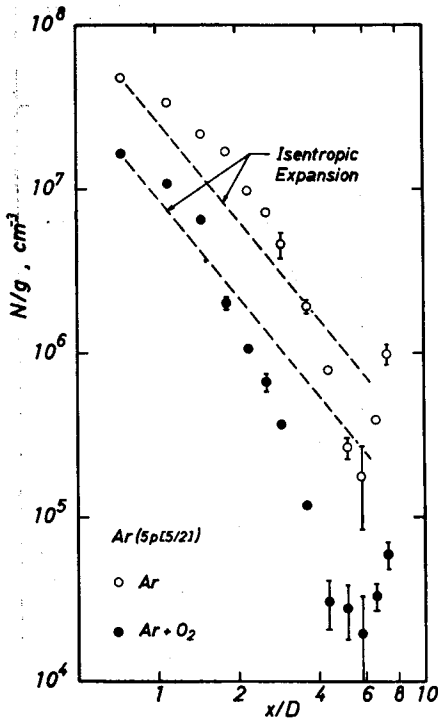
Fig. 6. Distribution of Ar(5p[5/2]) population
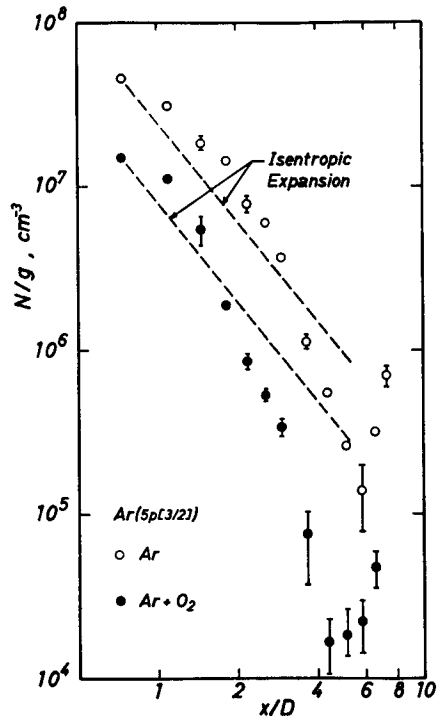density on the freejet centerline.

Fig. 7. Distribution of Ar(5p[3/2]) population
density on the freejet centerline.

to the Mach disk.

Figure 7 shows the population density variations of Ar(5p[3/2]), which has been determined from the measurement on the line of ArI 4159. The feature in this figure is very similar to that in Fig. 6.

3.4. Population Densities of O($3p^3P$) and O($3p^5P$)

The population densities of O($3p^3P$) and O($3p^5P$) are shown in Fig. 8. These population densities have been determined from the absolute intensity measurements of OI 8446 and OI 7773. The feature of this result is very similar to that of the argon, i. e. in the downstream a rapid decrease in the population density is also observed.

The experimental ratio of the population density N divided by the statistical weight g of the $3p^3P$ state to that of the $3p^5P$ state on the freejet centerline is shown in Fig. 9. Although the freejet pressure rapidly decreases with an increase in the distance as shown in Fig. 3, the ratio remains almost unchanged. Piper[10] showed that the ratio of the emission intensity from the $3p^5P$ state to that from the $3p^3P$ state
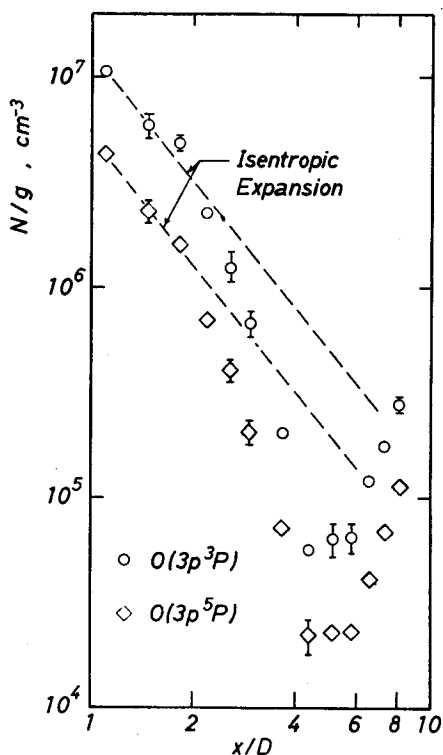
Fig. 8. Distribution of O($3p^3P$) and O($3p^5P$) populattion density on the freejet centerline.
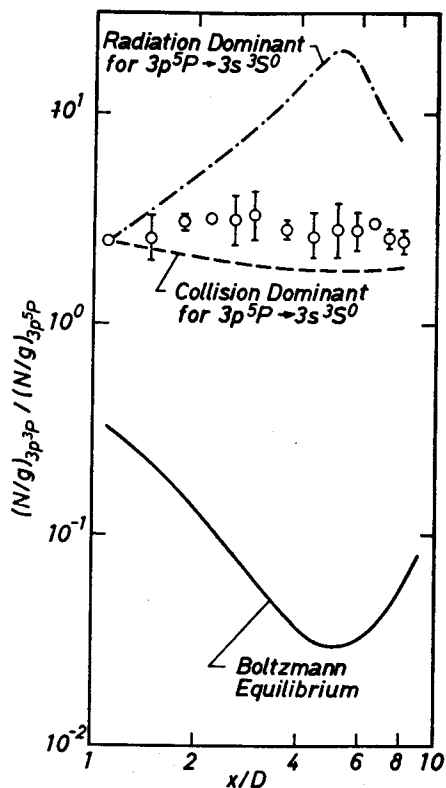

Fig. 9. Variation of the ratio [$N(3p^3P)$/ $g(3p^3P)$]/[$N(3p^5P)/g(3p^5P)$] in the supersonic freejet.

was pressure-dependent over the pressure range 67-530 Pa(0.5-4.0 Torr). In the present result the pressure-dependent ratio is not observed. Concerning this point, the present result does not agree with Piper's result. Hence, it may be mentioned that the $3p^5P$ state is populated by an electron-collisional de-excitation of O($3p^3P$) rather than by the quenching of O($3p^3P$) by ground state argon. The ratio $N(3p^3P)$/ [$g(3p^3P)$]/[$N(3p^5P)/g(3p^5P)$] has been estimated by assuming Boltzmann equilibrium between the $3p^3P$ and $3p^5P$ states at the local electron temperature measured by means of the electrostatic probe. The calculated result does not agree with the experimental one, so that these two states are not in the Boltzmann equilibrum. Since it is expected that the relaxation time of $3p^5P$ is much less than the characteristic flow time ($\simeq 10^{-5}$ sec), we introduce a steady state population of the $3p^5P$ state:

$$\dot{N}(3p^5P) = -N(3p^5P)[A+N_eQ(3p^5P{\rightarrow}3s^3S^0)]+N(3p^3P)N_eQ(3p^3P{\rightarrow}3p^5P)$$

$$=0, \hspace{5cm} (5)$$

where A is the Einstein A coefficient for a radiative de-excitation from the $3p^5P$ state and $Q(j{\rightarrow}k)$ the rate constant for an electron-collisional transition from the j-state to the k-state. Equation (5) gives

$$\frac{N(3p^3P)/g(3p^3P)}{N(3p^5P)/g(3p^5P)} = \frac{A+N_eQ(3p^5P{\rightarrow}3s^3S^0)}{N_eQ(3p^3P{\rightarrow}3p^5P)}\ \frac{g(3p^5P)}{g(3p^3P)}. \tag{6}$$

We assume that a Thomson formula[11] for the cross section of electron-collisional excitation can be applied to the oxygen atom. Then we have the following de-excitation rate constant:

$$Q(j{\rightarrow}k) = 5.45K(j{\rightarrow}k)T_e^{-1.5}[g(k)/g(j)]/[u_{j,k}(u_{j,k}+1)]\ \text{cm}^3\ \text{sec}^{-1}, \tag{7}$$

where $u_{j,k}=E_{j,k}/\tilde{k}T_e$, $E_{j,k}$ is the energy difference beteen the j-state and k-state, T_e the electron temperature, $\tilde{k}$ the Boltzmann constant and $K(j{\rightarrow}k)$ the parameter to achieve numerical agreement with experiment. When $K(j{\rightarrow}k)=1$, it follows that $Q(3p^3P{\rightarrow}3p^5P)=2.97\times10^{-5}\ \text{cm}^3\ \text{sec}^{-1}$ and $Q(3p^5P{\rightarrow}3s^3S^0)=2.46\times10^{-7}\ \text{cm}^3\ \text{sec}^{-1}$ at $x/D=1.1$.

According to Eq. (6) the ratio $[N(3p^3P)/g(3p^3P)]/[N(3p^5P)/g(3p^5P)]$ has been calculated by employing the measured electron temperature and density. The chain curve in Fig. 9 represents the result calculated in the case when $A{\gg}N_eQ(3p^5P{\rightarrow}3s^3S^0)$, i. e. the radiation dominant case. It seems impossible to explain the experimental result with this prediction. The dashed curve indicates the case when $N_eQ(3p^5P{\rightarrow}3s^3S^0){\gg}A$, i. e. the collision-dominant case. In this case, the value of the ratio $K(3p^5P{\rightarrow}3s^3S^0)/K(3p^3P{\rightarrow}3p^5P)$ has been determined by fitting the calculated ratio of $[N(3p^3P)/g(3p^3P)]/[N(3p^5P)/g(3p^5P)]$ for the experimental ratio at $x/D=1.1$. Its magnitude is 176. Although the calculated result deviates slightly from the experimental one, this prediction agrees well with the experiment as regards the the fact that the ratio $[N(3p^3P)/g(3p^3P)]/[N(3p^5P)/g(3p^5P)]$ remains almost unchanged over the freejet expansion region.

4. Concluding Remarks

For the purpose of producing atomic oxygen, oxygen gas has been seeded into preionized argon plasma. As predicted, the lines 8446 A and 7773 A of the atomic oxygen have been observed. The comparisons of the electron temperature, electron density and argon population density in the cases of the pure Ar plasma and the O_2-seeded Ar plasma show that the plasma decays by seeding the oxygen gas.

From the comparison of the experimental and predicted results of the population densities of $O(3p^3P)$ and $O(3p^5P)$, the following might be mentioned on the condition that $N_e=1.8\times10^{13}-1.7\times10^{12}\text{cm}^{-3}$, $T_e=3000-900K$ and $p=48-0.19\ \text{Pa}(0.36-0.0014\ \text{Torr})$: The $3p^5P$ state is populated by the electron-collisional de-excitation of the

$3p^3P$ state, rather than by the quenching of the $3p^3P$ state by the ground state argon. The $3p^5P$ state is de-populated by the electron-collisional de-excitation rather than by radiative de-excitation.

References

1) W. R. Bennett, Jr., W. L. Faust, R. A. McFarlane and C. K. N. Patel, Phys. Rev. Letters 8, 470 (1962).
2) W. H. Breckenridge and T. A. Miller, Chem. Phys. Letters 12, 437 (1972).
3) D. L. King, L. G. Piper and D. W. Setser, J. Chem. Soc. Farady Trans. II 73, 177 (1977).
4) M. Nishida, Doctral Thesis, Kyoto University (1969).
5) J. W. Tukey, Proceedings of the Conference on Critical Evaluation of Chemical Physical Structual Information, 1974, p. 3 and p. 48.
6) H. R. Griem, Plasma Spectroscopy (McGraw-Hill, New York 1964) p. 176.
7) R. B. Larrabee, J. Opt. Soc. Am. 49, 619 (1959).
8) P. E. Cassady and L. Lees, AIAA J. (Am. Inst. Aeronaut. Astronaut.) 10, 855 (1972).
9) A. Kimura nad M. Nishida, Trans. Japan Soc. Aeronaut. Space Sci. 22, 162 (1979).
10) L. G. Piper, Chem. Phys. Letters 28, 276 (1974).
11) E. Hinnov and J. G. Hirschberg, Proceedings of the Fifth International Conference on Ionized Phenomena in Gases, Vol. I, edited by H. Maecker, (North-Holland, Amsterdam, 1962) p. 638.